FUDMA Journal of Sciences (FJS)
ISSN online: 2616-1370
ISSN print: 2645 - 2944
Vol. 10 No. 3, February, 2026, pp 69 – 78
DOI: https://doi.org/10.33003/fjs-2026-1003-4744

DYNAMIC ANALYSIS OF A NON-PRISMATIC DAMPED CANTILEVER THIN BEAM RESTING ON AN EXPONENTIALLY DECAYING ELASTIC FOUNDATION UNDER CONSTANT AND HARMONIC DISTRIBUTED LOADS

***[1]Taiwo Aanu Ogunlusi, [2]Lawrence Osa Adoghe, [3]Adamu Bala, [4]Ezekiel Olaoluwa Omole, [5]Folasade Helen Odeniyan-Fakuade and [6,7]Taiwo Stephen Fayose**

[1]Department of Mathematics, Federal University Oye-Ekiti, Ekiti State, Nigeria
[2]Department of Mathematics, Ambrose Alli University, Ekpoma, Edo State, Nigeria
[3]Department of Basic Sciences, Auchi Polytechnic, Auchi, Edo State, Nigeria
[4]Department of Mathematics, Federal University of Technology and Environmental Sciences, Iyin Ekiti, Ekiti State, Nigeria
[5]Department of Mathematical Sciences, Osun State University, Osogbo, Osun State, Nigeria
[6]Department of Statistics, Federal Polytechnic Ado-Ekiti, Ekiti State, Nigeria
[7]Department of Statistics, Federal University of Technology and Environmental Sciences, Iyin-Ekiti, Ekiti State, Nigeria

*Corresponding authors' email: taiwo.ogunlusi@fuoye.edu.ng

ABSTRACT

This research examines the dynamic response of a non-prismatic damped cantilever thin beam (NPDCTB) under constant distributed load (CDL) and harmonic distributed load (HDL). The beam governing equation is a fourth-order partial differential equation (PDE), which is reduced into a second-order ordinary differential equation (ODE) using the generalized Galerkin method (GGM). The resulting ODEs are solved analytically for both loading cases using Laplace transforms (LT) and convolution theory (CT) to evaluate the transverse deflection of the NPDCTB. The effects of load speed c, axial force, damping coefficient, beam depth, and beam breadth on the dynamic response are examined and presented in the curve. The results showed the significant influence of cantilever boundary conditions on the vibration characteristics of non-prismatic beams under dynamic loading. The results demonstrate that load speed significantly amplifies the transverse deflection, while increases in axial force, damping coefficient, beam depth, and beam breadth lead to reductions in vibration amplitude.

Keyword: Constant Distributed Load, Harmonic Distributed Load, Exponentially Decaying Foundation, Cantilever Thin Beam

INTRODUCTION

This research builds on earlier work by (Ogunlusi & Okarfor, 2025) which investigates the vibration of a non-prismatic damped thin beam (NPDTB) with exponentially varying thickness resting on exponentially decaying foundations under uniform distributed loads. Thin beam (TB) is a structural component that mostly withstands loads applied laterally across its axis (Bauchau & Craig, 2009) It can be used in a variety of civil and aerospace engineering applications due to its strong stiffness and light weight. Non-prismatic thin beams (NPTB), sometimes referred to as beams with non-constant cross-sections or beams of variable cross-sections, are a specific class of thin bodies that are of interest to practitioners because of the potential to optimize their geometry in relation to particular needs (Timoshenko, 1965; Auricchio et al., 2015). Many researchers, such as Dado & Al-Sadder (2005), Hashim et al. (2022), Elshabrawy et al. (2021), Oyelami & Falodun (2021), and Ogbo et al. (2025), have worked on the NPB due to the variation of cross-sectional properties along its length, which has significantly affected its dynamic behavior.

Their studies showed that the NPTB model is a better representation of real-life engineering structures; as a result, they have attracted considerable attention from many authors in literature. Damping is an important parameter in structural dynamics, referring to the mechanism by which vibrational energy dissipates within a structure, thereby reducing the amplitude of oscillation and preventing excessive dynamic responses. (Inman, 2014; Clough & Penzien, 1993). The NPTB considered in this work is subjected to damping, which can have an effect on its dynamic behavior. The material (internal) damping, air resistance, structural damping, and some structural effects are the main causes of damping in the dynamics of a structure, and their influence in the dynamics of a structure must be carefully studied because they affect the vibrational response and stability of structural engineering systems. An analytic solution for a thin beam with non-proportional damping under a moving load developed by (Svedholm, 2016) provides knowledge into how the damping materials affect the beam structure. Additionally, (Praharaj & Datta, 2022) studied the response of a viscoelastic beam under dynamic loading using a fractional-order Kelvin-Voigt method, showing that the order of the fractional derivative strongly affects the natural frequencies and damping of the beam. Other researchers that worked on the dynamic behavior of NPTB with damping parameters, including the work of Jimoh & Ajoge (2018), Lei et al. (2013), Fadugba et al. (2022), Alimi & Adekunle (2018), Geraschenko et al. (2018) and Olotu et al. (2025). A cantilever beam is a rigid structural component that has one free end and one fixed end. This makes it possible to use cantilever beams in overhanging structures, allowing for the creation of an open area beneath the beam. In a study on cantilever beams, studied in Jassim et al., Wu & Chen (2002), Li et al. (2013), Al-Raheimy & Hammed (2022) Sarkar et al. (2016) and Omole et al. (2025). ,they worked on cantilever beams under various loading conditions. The NPDCTB in this research is subjected to exponentially decaying foundations. The exponentially decaying foundation diminishes exponentially with depth. Applications for this kind of foundation can be seen in offshore buildings, where the stiffness of the foundation diminishes with the depth as a result of the surrounding soil

decreasing in density. Research on the dynamic behavior of structures on exponentially decaying foundations has been investigated by Tolorunshagba (2014), Adekunle & Folakemi (2017), Jimoh & Ajoge (2019), Adedowole & Famuagun (2017), Okafor et al. (2025) and Sunday et al. (2026). The non-prismatic thin beam considered in this work is a cantilever beam, which is fixed at one end and free at the other. Previous studies investigate the vibration of non-prismatic damped simply supported thin beams with exponentially varying thickness resting on exponentially decaying foundations under uniform distributed loads by (Ogunlusi & Okarfor, 2025). There is a significant difference in the analysis of non-prismatic cantilever beams supported by exponentially decaying foundations, particularly under distributed constant and harmonic loads. Despite much research on non-prismatic beams, the case of a non-prismatic cantilever beam on a decaying foundation remains unknown, with a limited understanding of its dynamic response under different loading conditions.

Methodology

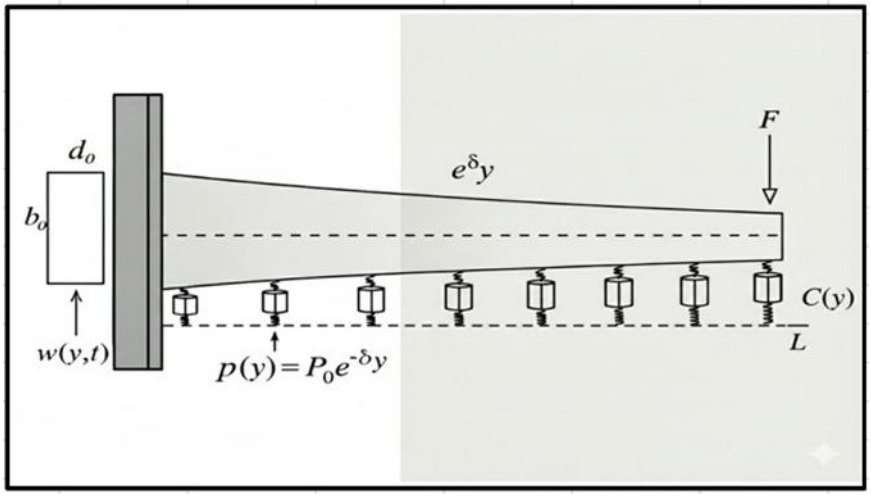

Figure 1: Geometry Representation of NPDCTB on Exponential Decaying Foundation

The dynamic behavior of an NPCTB with exponentially varying thickness, subject to distributed loads at constant velocity, and resting on an exponentially decaying foundation is described by the fourth-order PDE:

$$(\sigma A(y){D_t}^2 + C(y){D_t}^2 + L_y)w(y,t) = F(y,t). \quad (1)$$

Where L_y is the spatial differential operator defined by

$$L_y = P(y) + {D_y}^2(EI(y)){D_y}^2 + N_0{D_y}^2. \quad (2)$$

Table 1: Meaning of Symbol use in Governing Equation

Symbol	Meaning
σ	Density
A(y)	Variable Cross section area
$I(y)$	Variable Moment of inertia
$C(y)$	Variable Damping
$P(y)$	Exponential decaying foundation
N_0	Axial force
D_y	partial derivative in relation to the spatial coordinate y
D_t	Partial derivative in relation to time t
$w(y,t)$	Beam Displacement

Further simplification of equation (1), gives

$$\sigma A(y)w_{tt}(y,t) + C(y)w_t(y,t) + EI(y)w_{yyyyy}(y,t) + 2EI'(y)w_{yyy}(y,t) + EI''(y)w_{yy}(y,t) - N_0w_{yy}(y,t) + P(y)w(y,t) = F(y,t). \quad (3)$$

According to Ece et al. (2017) the variable moment of inertia $I(y)$ and cross section area A(y) of the beam can be represented in exponential form, the NPCTB has a constant breadth $b = b_0$and a depth that varies exponentially along its length (L), given by

$$d(y) = 2d_0exp^{\delta y}. \quad (4)$$

The beam area is given by

$$A(y) = bd(y) = 2b_0d_0exp^{\delta y}. \quad (5)$$

The TB's moment of inertia is expressed as

$$I(y) = \frac{1}{12}d^3b = d_0^3b_0exp^{3\delta y}. \quad (6)$$

The damping acting on the beam is modeled as

$$C(y) = bd(y)C_0\zeta \quad (7)$$

where d_0 and $b_0$denote the constant reference (initial) depth and breadth of the beam cross-section, ζ is the damping ratio and C_0 is the damping coefficient. For a critically damped system (ζ =1), this reduces to

$$C(y) = b_0d_0exp^{\delta y}C_0 \quad (8)$$

The exponential decay foundation is modeled as follows, using (Omolofe et al., 2011)

$$P(y) = P_0exp^{-\delta y} \quad (9)$$

We assumed the TB initial condition is given by

$$w(y,t)|_{t=0} = 0 = D_tw(y,t)|_{t=0}. \quad (10)$$

When equations (5)– (8) are substituted into equation (3), the result is

$exp^{3\delta y}(\frac{2E}{3}d_0^3b_0w_{yyyyy}(y,t)+4E\delta d_0^3b_0w_{yyy}(y,t)+6E\delta^2d_0^3b_0w_{yy}(y,t))-N_0w_{yy}(y,t)+P_0exp^{-\delta y}w(y,t)+2\sigma d_0b_0exp^{\delta y}(\sigma+C_0)w_{tt}(y,t)=F(x,t).$ (11)

CASE 1: NPDCTB Resting on an Exponentially Decaying Elastic Foundation under CDL

This section examines the dynamic response of an NPDCTB with exponentially varying thickness that is subjected to a CDL while resting on an exponentially decaying foundation, the applied load $F(y,t)$ is expressed as

$F(y,t)=F_0U(y-ct)$ (12)

Using equation (12) in equation (11), we have

$\sigma d_0b_0exp^{\delta y}(\sigma w_{tt}+C_0w_{tt})+exp^{3\delta y}(\frac{2E}{3}d_0^3b_0w_{yyyyy}+4E\delta d_0^3b_0w_{yyy}+6E\delta^2d_0^3b_0w_{yy})-N_0w_{yy}+P_0exp^{-\delta y}=F_0H(x-ct).$ (13)

The definition of the Heaviside function, represented by $U(y-ct)$, is

$$U(y-ct)=\begin{cases}0, & y<ct;\\ 1, & y\geq ct,\end{cases} \quad (14)$$

with the properties

$$\frac{d}{dy}\big(U(y-ct)\big)=\delta(x-ct)$$

$$u(y)U(y-ct)=\begin{cases}0, & y<ct;\\ u(y), & y>ct.\end{cases} \quad (15)$$

$$\int_0^L U(y-ct)f(y)\,dy=\int_{ct}^L f(y)\,dy,\ 0\leq ct\leq L \quad (16)$$

To obtain the closed-form solution of Equation (12), GGM developed by (Ojih *et al.*, 2014) is adopted, defined as:

$w(y,t)=\sum_{h=1}^{\infty}w_h^*(t)U_h^*(y).$ (17)

where $w_h^*(t)$ is the time dependent modal coordinates, $U_h^*(y)$ is the spatial normal mode shapes associated with the free vibration of the beam.

$U_h^*(y)=\sin\frac{\theta_hy}{L}+A_h\cos\frac{\theta_hy}{L}+B_h\sinh\frac{\theta_hy}{L}+C_h\cosh\frac{\theta_hy}{L}.$ (18)

The constants A_h, B_h, and C_h describe the vibration amplitude and mode shape and the value depend on the boundary conditions.

Equation (17) is substituted into equation (13), and after simplification, gives $\sum_{h=1}^{\infty}\{exp^{\delta y}(U_h^*(y)\ddot{w}_h^*(t)+\frac{C_0}{\sigma}U_h^*(y)\dot{w}_h^*(t))+exp^{3\delta y}\left(\left(\frac{2E}{3\sigma}\right)U_h^{*iv}(y)-\left(\frac{2Ed_0^2\delta}{\sigma}\right)U_h^{*\prime\prime\prime}(y)\right)-\left(\frac{3Ed_0^2\delta^2}{\sigma}\right)U_h^{*\prime\prime}(y)\Big)+\left(\frac{N}{2\sigma d_0b_0}\right)U_h^{*\prime\prime}(y)+\frac{P_0}{2\sigma d_0b_0}e^{-\delta y}U_h^*(y)\}w_h^*(t)\frac{F_0}{2\sigma d_0b_0}U(y-ct)\}=0$. (19)

Equation (19) is orthogonalized with respect to $U_\alpha^*(y)$ in order to solve $w_h^*(t)$

Where

$U_\alpha^*(y)=sin\frac{\theta_\alpha y}{L}+A_\alpha cos\frac{\theta_\alpha y}{L}+B_\alpha sinh\frac{\theta_\alpha y}{L}+C_\alpha cosh\frac{\theta_\alpha y}{L}$ (20)

$\int_0^L\sum_{h=1}^{N}\left\{exp^{\delta y}\left(U_h^*(y)\ddot{w}_h^*(t)+\frac{C_0}{\sigma}U_h^*(y)\dot{w}_h^*(t)\right)+\left(exp^{3\delta y}\left(\left(\frac{2E}{3\sigma}\right)U_h^{*iv}(y)+\left(\frac{2Ed_0^2\delta}{\sigma}\right)U_h^{*\prime\prime\prime}(y)\right)+\left(\frac{3Ed_0^2\delta^2}{\sigma}\right)U_h^{*\prime\prime}(y)\right)+\left(\frac{N}{2\sigma d_0b_0}\right)U_h^{*\prime\prime}(y)+\frac{P_0}{2\sigma d_0b_0}e^{-\delta y}U_h^*(y)\right)w_h^*(t)-\frac{F_0}{2\sigma d_0b_0}U(y-ct)\Big\}U_\alpha^*(y)dy=0$ (21)

Simplification and rearrangement of equation (21) yield

$\lambda_1\ddot{w}_h^*(t)+\lambda_2\dot{w}_h^*(t)+(\lambda_3-\lambda_4-\lambda_5-\lambda_6+\lambda_7)w_h^*(t)=F_h\lambda_8$. (22)

Where

$F_h=\frac{F_0}{2\sigma d_0b_0}$

$\lambda_1=\int_0^L exp^{\delta y}\,U_\alpha^*(y)\,U_h^*(y)dy$

$\lambda_2=\frac{C_0}{\sigma}\int_0^L exp^{\delta y}\,U_\alpha^*(y)U_h^*(y)dy$

$\lambda_3=\frac{2E}{3\sigma}\int_0^L exp^{3\delta y}\,U_\alpha^*(y)\,U_h^{*iv}(y)dy$

$\lambda_4=\frac{2Ed_0^2\delta}{\sigma}\int_0^L exp^{3\delta y}\,U_\alpha^*(y)U_h^{*\prime\prime\prime}(y)dy$

$\lambda_5=\frac{3Ed_0^2\delta^2}{\sigma}\int_0^L exp^{3\delta y}\,U_\alpha^*(y)U_h^{*\prime\prime}(y)dy$

$\lambda_6=\frac{N}{2\sigma d_0b_0}\int_0^L exp^{3\delta y}\,U_\alpha^*(y)U_h^{*\prime\prime}(y)dy$

$\lambda_7=\frac{P_0}{2\sigma d_0b_0}\int_0^L exp^{-\delta y}\,U_\alpha^*(y)U_h^*(y)dy.$ (23)

$\lambda_8=\int_0^L U(y-ct)U_\alpha^*(y)dy.$ (24)

The beam is modeled is a cantilever thin beam. Accordingly, the boundary conditions are in the form

$w(y,t)|_{y=0}=0=D_yw(y,t)|_{y=0}$,

and $D_y{}^2w(y,t)|_{y=L}=0=D_y{}^3w(y,t)|_{y=L}$. (25)

using the boundary condition in equation (20), it is easier to show that.

$A_\alpha=-\frac{\sin\theta_\alpha+\sinh\theta_\alpha}{\cos\theta_\alpha+\cosh\theta_\alpha}=\frac{\cosh\theta_\alpha+\cos\theta_\alpha}{\sin\theta_\alpha-\sinh\theta_\alpha}=-C_\alpha$ (26)

and $B_k=-1.$ (27)

And the frequency equation for both end conditions is

$\cos a_\alpha\cosh a_\alpha=-1$ (28)

substituting equation (26) and (27) in equation (20), it gives

$U_\alpha^*(y)=sin\frac{\theta_\alpha y}{L}-sinh\frac{\theta_\alpha y}{L}+A_\alpha\left(cos\frac{\theta_\alpha y}{L}-cosh\frac{\theta_\alpha y}{L}\right)$ (29)

Evaluate the integral in equation (24) using the properties of The Heaviside function is defined in equation (14); equation (28)

$\lambda_1\ddot{w}_h^*(t)+\lambda_2\dot{w}_h^*(t)+\lambda_{21}w_h^*(t)=\frac{LF_h}{\theta_\alpha}(\theta_{\alpha C}+\cos\phi t+\cosh\phi t+A_\alpha(-\sinh\phi t+sin\phi t)$ (30)

Where

$\theta_{\alpha C}=-\cos\theta_\alpha-\cosh\theta_\alpha+A_\alpha(\sin\theta_\alpha-\sinh\theta_\alpha)$ and $\phi=\frac{\theta_\alpha}{L}$. (31)

Equation (22) can be further simplified to obtain

$\ddot{w}_h^*(t)+E_1\dot{w}_h^*(t)+E_2w_h^*(t)=E_h(\theta_{\alpha C}+\cos\phi t+\cosh\phi t+A_\alpha(-\sinh\phi t+sin\phi t)$. (32)

Where

$E_1=\frac{\lambda_2}{\lambda_1}$, $E_2=\frac{\lambda_3}{\lambda_1}$ and $E_h=\frac{LF_h}{\theta_\alpha\lambda_1}$. (33)

Equation (32) represents a reduce second-order ODE, which can be solved using the LT method. The LT of a function $\boldsymbol{w_h^*(t)}$ is defined as

$L\{w_h^*(t)\}=\int_0^\infty w_h^*(t)\,e^{-St}$ (34)

Applying the LT together with the initial conditions defined in equation (10) gives

$(S^2+SE_1+E_2)w_h^*(s)=E_h(\frac{\theta_{\alpha C}}{S}+\frac{S}{S^2+\phi^2}+\frac{S}{S^2-\phi^2}-A_\alpha\left(\frac{\phi}{S^2+\phi^2}+\frac{\phi}{S^2-\phi^2}\right)$.

(35)

Simplifying equation (35) further yields

$w_h^*(s)=\frac{E_h}{(S-v_1)(S-v_2)}(\frac{\theta_{\alpha C}}{S}+\frac{S}{S^2+\phi^2}+\frac{S}{S^2-\phi^2}+A_\alpha\left(\frac{\phi}{S^2+\phi^2}-\frac{\phi}{S^2-\phi^2}\right)$ (36)

Where

$$v_{1,2} = -\frac{\sigma_1}{2} \pm \frac{\sqrt{E_1^2-4E_2}}{2} \quad (37)$$

To obtain the inverse LT of equation (29), we will utilize the following representation

$$F(S) = \frac{1}{(S-v_1)(S-v_2)}, \quad G(S) = \frac{\theta_{\alpha C}}{S} + \frac{S}{S^2+\phi^2} + \frac{S}{S^2-\phi^2} + A_\alpha\left(\frac{\phi}{S^2+\phi^2} - \frac{\phi}{S^2-\phi^2}\right). \quad (38)$$

The inverse LT of Equation (26) can be represented as the CT of F and G, expressed as:

$$F * G = \int_0^t F(t-\xi)G(\xi)d\xi \quad (39)$$

the inverse LT of Equation (26) is written in the form

$$w_h^*(t) = \frac{E_h}{(v_1-v_2)}(\theta_{\alpha C}J_1 + J_2 + J_3 + A_\alpha(J_4 - J_5) - \theta_{\alpha C}J_6 - J_7 - J_8 - A_\alpha(J_9 + J_{10})). \quad (40)$$

where

$$J_1 = \int_0^t exp^{v_1(t-\xi)}d\xi$$
$$J_2 = \int_0^t exp^{v_1(t-\xi)}\cos\phi\xi d\xi$$
$$J_3 = \int_0^t exp^{v_1(t-\xi)}\cosh\phi\xi d\xi$$
$$J_4 = \int_0^t exp^{v_1(t-\xi)}\sin\phi\xi d\xi$$
$$J_5 = \int_0^t exp^{v_2(t-\xi)}\sinh\phi\xi d\xi$$
$$J_6 = \int_0^t exp^{v_1(t-\xi)}d\xi$$
$$J_7 = \int_0^t exp^{v_2(t-\xi)}\cos\phi\xi d\xi$$
$$J_8 = \int_0^t exp^{v_2(t-\xi)}\cosh\phi\xi d\xi$$
$$J_9 = \int_0^t exp^{v_2(t-\xi)}\sin\phi\xi d\xi$$
$$J_{10} = \int_0^t exp^{v_2(t-\xi)}\sinh\phi\xi d\xi \quad (41)$$

Solving the integral in equation (41) and substitute in to equation (40), gives

$$w_h^*(t) = \frac{E_h}{(v_1-v_2)}\left\{\left(\theta_{\alpha C}\frac{exp^{v_1 t}-1}{v_1} + \frac{1}{\phi^2+v_1^2}(\phi\sin\phi t - v_1\cos\phi t + v_1 exp^{v_1 t}) + \frac{1}{\phi^2-v_1^2}(\phi\sinh\phi t + v_1\cosh\phi t - v_1 exp^{v_1 t}) + A_\alpha\left(\frac{1}{\phi^2+v_1^2}(-\phi\cos\phi t - v_1\sin\phi t + v_1 exp^{v_1 t}) - \frac{1}{\phi^2-v_1^2}(\phi\cosh\phi t + v_1\sinh\phi t - v_1 exp^{v_1 t})\right)\right) - \left(\theta_{\alpha C}\frac{exp^{v_2 t}-1}{v_2} + \frac{1}{\phi^2+v_2^2}(\phi\sin\phi t - v_2\cos\phi t + v_2 exp^{v_2 t}) + \frac{1}{\phi^2-v_2^2}(\phi\sinh\phi t + v_2\cosh\phi t - v_2 exp^{v_1 t}) + A_\alpha\left(\frac{1}{\phi^2+v_2^2}(-\phi\cos\phi t - v_2\sin\phi t + v_2 exp^{v_2 t}) - \frac{1}{\phi^2-v_2^2}(\phi\cosh\phi t + v_2\sinh\phi t - v_2 exp^{v_2 t})\right)\right)\right\} \quad (42)$$

Inserting equation (42) into equation (17) yields:

$$w(y,t) = \sum_{h=1}^{\infty}\frac{E_h}{(v_1-v_2)}\left\{\left(\theta_{\alpha C}\frac{exp^{v_1 t}-1}{v_1} + \frac{1}{\phi^2+v_1^2}(\phi\sin\phi t - v_1\cos\phi t + v_1 exp^{v_1 t}) + \frac{1}{\phi^2-v_1^2}(\phi\sinh\phi t + v_1\cosh\phi t - v_1 exp^{v_1 t}) + A_\alpha\left(\frac{1}{\phi^2+v_1^2}(-\phi\cos\phi t - v_1\sin\phi t + v_1 exp^{v_1 t}) - \frac{1}{\phi^2-v_1^2}(\phi\cosh\phi t + v_1\sinh\phi t - v_1 exp^{v_1 t})\right)\right) - \left(\theta_{\alpha C}\frac{exp^{v_2 t}-1}{v_2} + \frac{1}{\phi^2+v_2^2}(\phi\sin\phi t - v_2\cos\phi t + v_2 exp^{v_2 t}) + \frac{1}{\phi^2-v_2^2}(\phi\sinh\phi t + v_2\cosh\phi t - v_2 exp^{v_1 t}) + A_\alpha\left(\frac{1}{\phi^2+v_2^2}(-\phi\cos\phi t - v_2\sin\phi t + v_2 exp^{v_2 t}) - \frac{1}{\phi^2-v_2^2}(\phi\cosh\phi t + v_2\sinh\phi t - v_2 exp^{v_2 t})\right)\right)\right\} \times \sin\frac{\theta_\alpha y}{L} + A_\alpha\cos\frac{\theta_\alpha y}{L} + B_\alpha\sinh\frac{\theta_\alpha y}{L} + C_\alpha\cosh\frac{\theta_\alpha y}{L}. \quad (43)$$

Equation (43) described transverse deflection of NPDCTB with exponentially varying thickness that is supported by an exponentially decaying foundation and subjected to a CDL

CASE 2: NPDCTB Resting on an Exponentially Decaying Elastic Foundation under HDL.

This section examines the dynamic response of an NPDCTB with exponentially varying thickness that is subjected to a HDL while resting on an exponentially decaying foundation. The applied load $F(y,t)$, is expressed as

$$F(y,t) = F_0\cos t\Omega U(y-ct) \quad (44)$$

Where Ω denotes the angular frequency of the applied harmonic distributed load.

$$2\sigma d_0 b_0 exp^{\delta y}(\sigma w_{tt} + C_0 w_{tt}) + exp^{3\delta y}(\frac{2E}{3}d_0^3 b_0 w_{yyyyy} + 4E\delta d_0^3 b_0 w_{yyy} + 6E\delta^2 d_0^3 b_0 w_{yy}) - N_0 w_{yy} + P_0 exp^{-\delta y} = F_0\cos t\Omega U(y-ct). \quad (45)$$

By comparing Equation (45) with Equation (13), it is straightforward to show that Equation (45) reduces to

$$\ddot{w}_h^*(t) + E_1\dot{w}_h^*(t) + E_2 w_h^*(t) = \cos t\Omega E_h(\theta_{\alpha C} + \cos\phi t + \cosh\phi t + A_\alpha(-\sinh\phi t + \sin\phi t)) \quad (46)$$

Equation (46) is analogous to equation (32), thus subjecting equation (46) to LT in conjunction with the initial conditions defined in equation (10) and using CT, we obtain

$$w_h^*(t) = \frac{E_h}{2(v_1-v_2)}\left\{\frac{2\theta_{\alpha C}}{\Omega^2+v_1^2}(\Omega\sin\Omega t - v_1\cos\Omega t + v_1 exp^{v_1 t}) + \frac{1}{\Psi_1^2+v_1^2}(\Psi_1\sin\theta_1 t - v_1\cos\Psi_1 t + v_1 exp^{v_1 t}) + \frac{1}{\Psi_2^2+v_1^2}(\Psi_2\sin\Psi_2 t - v_1\cos\Psi_2 t + v_1 exp^{v_1 t}) + \frac{1}{\Omega^2+\Phi_1^2}(\Omega\sin\Omega t\, exp^{\phi t}\Phi_1\cos\Omega t exp^{\phi t} - \Phi_1 exp^{v_1 t}) + \frac{1}{\Omega^2+\Phi_2^2}(\Omega\sin\Omega t\, exp^{-\phi t} - \Phi_2\cos\Omega t\, exp^{-\phi t} + \Phi_2 exp^{v_1 t}) - A_\alpha\left(\frac{1}{\Psi_1^2+v_1^2}(-\Psi_1\cos\Psi_1 t - v_1\sin\Psi_1 t + v_1 exp^{v_1 t}) + \frac{1}{\Psi_2^2+v_1^2}(-\Psi_2\cos\Psi_2 t - v_1\sin\Psi_2 t + v_1 exp^{v_1 t}) + \frac{1}{\Omega^2+\Phi_1^2}(\Omega\sin\Omega t\, exp^{\phi t} + \Phi_1\cos\Omega t exp^{\phi t} - \Phi_1 exp^{v_1 t}) - \frac{1}{\Omega^2+\Phi_2^2}(\Omega\sin\Omega t\, exp^{-\phi t} - \Phi_2\cos\Omega t\, exp^{-\phi t} + \Phi_2 exp^{v_1 t})\right) - \frac{2\theta_{\alpha C}}{\Omega^2+v_2^2}(\Omega\sin\Omega t - v_2\cos\Omega t + v_2 exp^{v_2 t}) -$$

$\frac{1}{\Psi_1^2+v_2^2}(\Psi_1\sin\theta_1 t - v_2\cos\Psi_1 t + v_2 exp^{v_2 t}) + \frac{1}{\Psi_2^2+v_2^2}(\Psi_2\sin\Psi_2 t - v_2\cos\Psi_2 t + v_2 exp^{v_2 t}) - \frac{1}{\Omega^2+\Phi_3^2}\big(\Omega\sin\Omega t\, exp^{\phi t} + \Phi_3\cos\Omega t exp^{\phi t} - \Phi_3 exp^{v_2 t}\big) - \frac{1}{\Omega^2+\Phi_4^2}\big(\Omega\sin\Omega t\, exp^{-\phi t} - \Phi_4\cos\Omega t\, exp^{-\phi t} + \Phi_4 exp^{v_2 t}\big) - A_\alpha\Big(\frac{1}{\Psi_1^2+v_2^2}(-\Psi_1\cos\Psi_1 t - v_2\sin\Psi_1 t + v_2 exp^{v_2 t}) - \frac{1}{\Psi_2^2+v_2^2}(-\Psi_2\cos\Psi_2 t - v_2\sin\Psi_2 t + v_2 exp^{v_2 t}) - \frac{1}{\Omega^2+\Phi_3^2}\big(\Omega\sin\Omega t\, exp^{\phi t} + \Phi_3\cos\Omega t exp^{\phi t} - \Phi_3 exp^{v_2 t}\big) + \frac{1}{\Omega^2+\Phi_4^2}\big(\Omega\sin\Omega t\, exp^{-\phi t} - \Phi_4\cos\Omega t\, exp^{-\phi t} + \Phi_4 exp^{v_2 t}\big)\Big)\Big\} \times \sin\frac{\theta_h y}{L} + A_h\cos\frac{\theta_h y}{L} + B_h\sinh\frac{\theta_h y}{L} + C_h\cosh\frac{\theta_h y}{L}$

(47)

$\Psi_1 = \mathrm{S} - \phi$, $\Psi_2 = \mathrm{S} + \phi$, $\Phi_1 = \phi - v_1$, $\Phi_2 = v_1 + \phi$, $\Phi_3 = \phi - v_2$ and $\Phi_4 = v_2 + \phi$

Inserting equation (47) into equation (17) yields

$w(y,t) = \sum_{h=1}^{\infty}\frac{E_h}{2(v_1-v_2)}\Big\{\frac{2\theta_\alpha c}{\Omega^2+v_1^2}(\Omega\sin\Omega t - v_1\cos\Omega t + v_1 exp^{v_1 t}) + \frac{1}{\Psi_1^2+v_1^2}(\Psi_1\sin\theta_1 t - v_1\cos\Psi_1 t + v_1 exp^{v_1 t}) + \frac{1}{\Psi_2^2+v_1^2}(\Psi_2\sin\Psi_2 t - v_1\cos\Psi_2 t + v_1 exp^{v_1 t}) + \frac{1}{\Omega^2+\Phi_1^2}\big(\Omega\sin\Omega t\, exp^{\phi t}\Phi_1\cos\Omega t exp^{\phi t} - \Phi_1 exp^{v_1 t}\big) + \frac{1}{\Omega^2+\Phi_2^2}\big(\Omega\sin\Omega t\, exp^{-\phi t} - \Phi_2\cos\Omega t\, exp^{-\phi t} + \Phi_2 exp^{v_1 t}\big) - A_\alpha\Big(\frac{1}{\Psi_1^2+v_1^2}(-\Psi_1\cos\Psi_1 t - v_1\sin\Psi_1 t + v_1 exp^{v_1 t}) + \frac{1}{\Psi_2^2+v_1^2}(-\Psi_2\cos\Psi_2 t - v_1\sin\Psi_2 t + v_1 exp^{v_1 t}) + \frac{1}{\Omega^2+\Phi_1^2}\big(\Omega\sin\Omega t\, exp^{\phi t} + \Phi_1\cos\Omega t exp^{\phi t} - \Phi_1 exp^{v_1 t}\big) - \frac{1}{\Omega^2+\Phi_2^2}\big(\Omega\sin\Omega t\, exp^{-\phi t} - \Phi_2\cos\Omega t\, exp^{-\phi t} + \Phi_2 exp^{v_1 t}\big)\Big) - \frac{2\theta_\alpha c}{\Omega^2+v_2^2}(\Omega\sin\Omega t - v_2\cos\Omega t + v_2 exp^{v_2 t}) - \frac{1}{\Psi_1^2+v_2^2}(\Psi_1\sin\theta_1 t - v_2\cos\Psi_1 t + v_2 exp^{v_2 t}) + \frac{1}{\Psi_2^2+v_2^2}(\Psi_2\sin\Psi_2 t - v_2\cos\Psi_2 t + v_2 exp^{v_2 t}) - \frac{1}{\Omega^2+\Phi_3^2}\big(\Omega\sin\Omega t\, exp^{\phi t} + \Phi_3\cos\Omega t exp^{\phi t} - \Phi_3 exp^{v_2 t}\big) - \frac{1}{\Omega^2+\Phi_4^2}\big(\Omega\sin\Omega t\, exp^{-\phi t} - \Phi_4\cos\Omega t\, exp^{-\phi t} + \Phi_4 exp^{v_2 t}\big) - A_\alpha\Big(\frac{1}{\Psi_1^2+v_2^2}(-\Psi_1\cos\Psi_1 t - v_2\sin\Psi_1 t + v_2 exp^{v_2 t}) - \frac{1}{\Psi_2^2+v_2^2}(-\Psi_2\cos\Psi_2 t - v_2\sin\Psi_2 t + v_2 exp^{v_2 t}) - \frac{1}{\Omega^2+\Phi_3^2}\big(\Omega\sin\Omega t\, exp^{\phi t} + \Phi_3\cos\Omega t exp^{\phi t} - \Phi_3 exp^{v_2 t}\big) + \frac{1}{\Omega^2+\Phi_4^2}\big(\Omega\sin\Omega t\, exp^{-\phi t} - \Phi_4\cos\Omega t\, exp^{-\phi t} + \Phi_4 exp^{v_2 t}\big)\Big)\Big\} \times \sin\frac{\theta_h y}{L} + A_h\cos\frac{\theta_h y}{L} + B_h\sinh\frac{\theta_h y}{L} + C_h\cosh\frac{\theta_h y}{L}$

(48)

Equation (48) described transverse deflection of NPDCTB with exponentially varying thickness that is supported by an exponentially decaying foundation and subjected to a constant distributed

RESULTS AND DISCUSSION

Table 2: NPDCTB Parameters For Numerical Result

Parameter	Value/ Range
Elastic modulus (E)	2.109 x 10^9N/m^2
Density (σ)	7850 kg/m^3
Span length *(L)*	12.192m
Moment of inertia (I)	2.877 x 10^{-3} kg/m^2
Axial force (N)	100000- 800000N
Damping coefficient (C)	200- 800 kg/m^2
Beam depth (d_0)	0.300- 0.750m
Beam breath (b_0)	0.150- 0.300m
Foundation modulus (F_0)	1000000 kg/m^2
Speed (c)	8.120m/s

Figure 2 shows the deflection of an NPDCTB on an exponentially decaying foundation under CDL; increasing the load speed c amplifies the deflection, with similar trends seen in Figure 3 under HDL. Also, Figures 4 and 5 showed the dynamic response of NPDCTB under CDL and HDL, respectively. Both show that increasing the axial force N_0 leads to a decrease in the beam's response amplitude. An increase in the damping coefficient C_0 decreases the deflection of the NPDCTB on an exponentially decaying foundation, as shown in Figure 6 for CDL and Figure 7 for HDL. An increase in beam depth $d_0$reduces the deflection of NPDCTB for both CDL and HDL, as shown in figures 8 and 9. Similarly, an increase in beam breath b_0 decreases the deflection of NPDCTB for both CDL and HDL, as shown in figures 10 and 11. Lastly, Figure 12 presents a comparison between the CDL and the HDL.

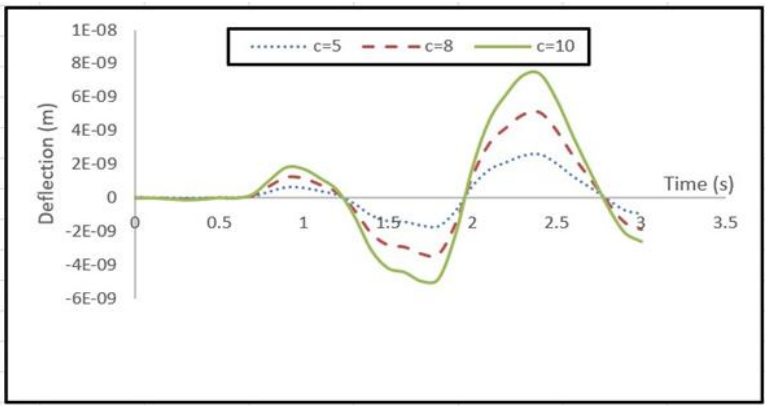

Figure 2: NPDCTB Deflection Profile under CDL for Various Speed c Values

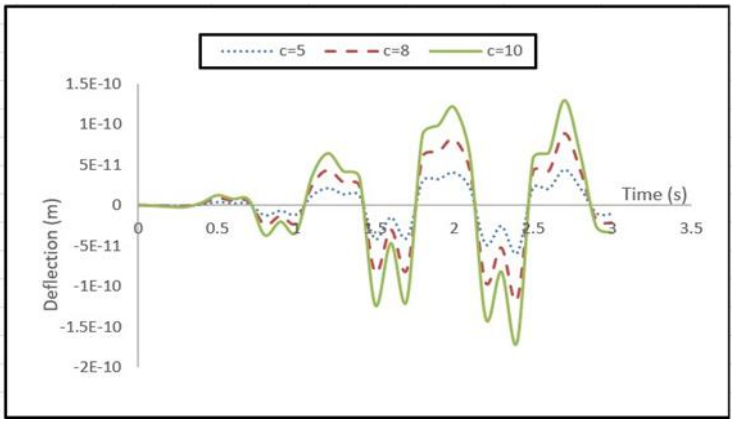

Figure 3: NPDCTB Deflection Profile under HDL for Various Speed c Value

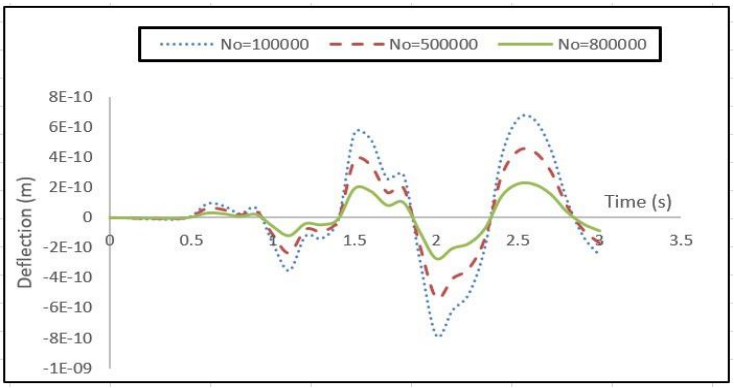

Figure 4: NPDCTB Deflection Profile under CDL for Various Axial force $\boldsymbol{N_0}$ Values

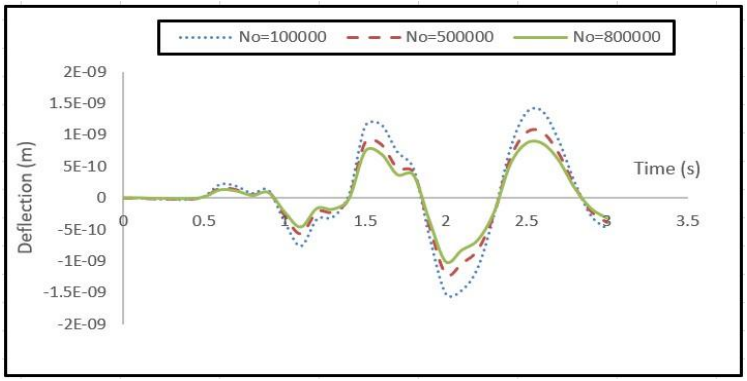

Figure 5: NPDCTB Deflection Profile under HDL for Various Axial force $\boldsymbol{N_0}$ Values

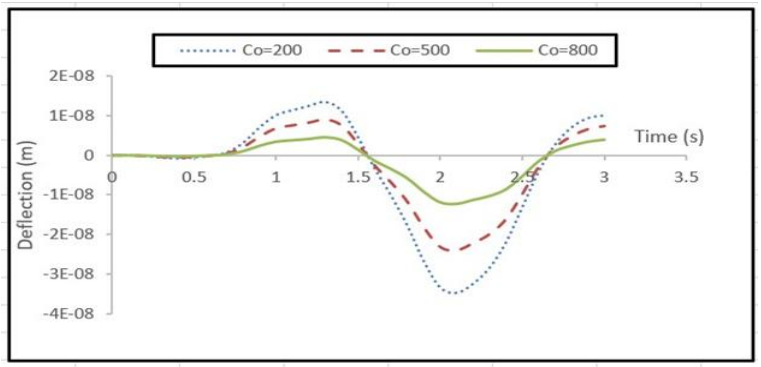

Figure 6: NPDCTB deflection Profile under CDL for Various Damping Coefficient C_0 Values

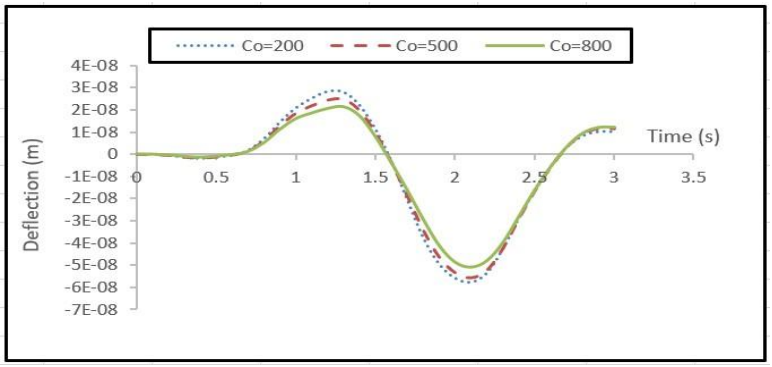

Figure 7 NPDCTB Deflection Profile under HDL for Various Damping Coefficient C_0Values

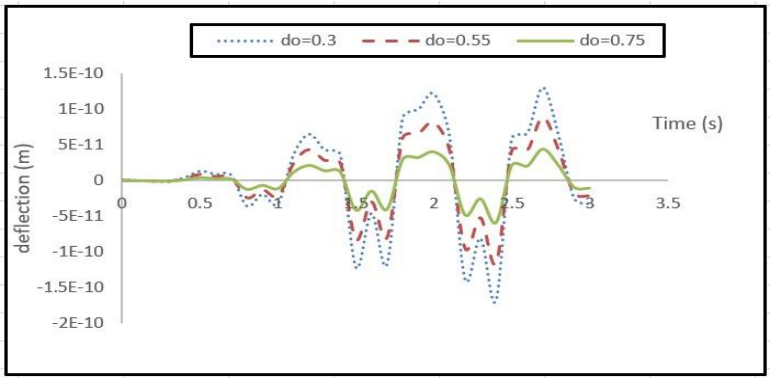

Figure 8: NPDCTB Deflection Profile under CDL for Various Beam Depth d_0 Values

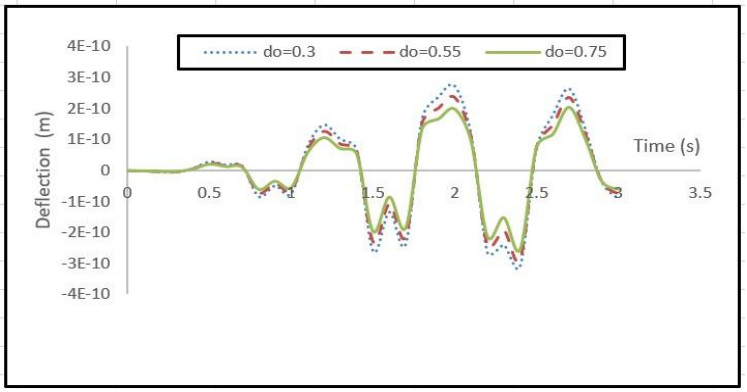

Figure 9: NPDCTB Deflection Profile under HDL for Various Beam Depth d_0 Values

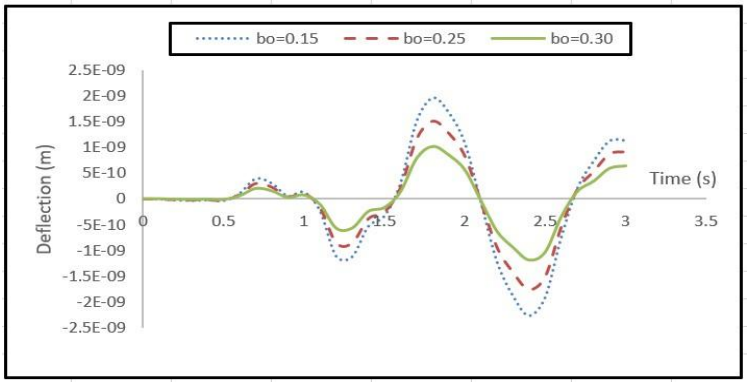

Figure 10: NPDCTB Deflection Profile under CDL for Various Beam Breath b_0 Values

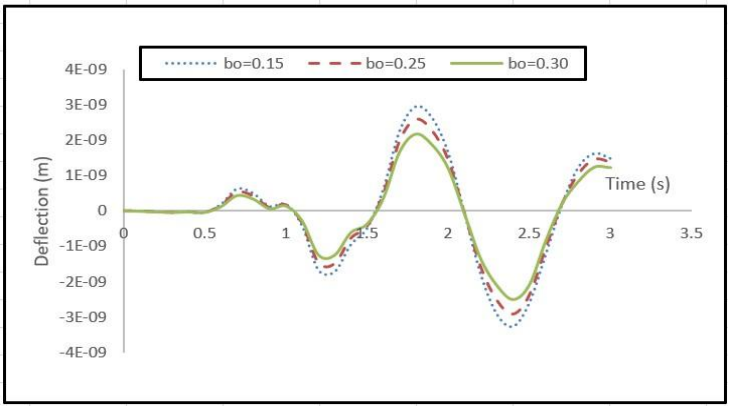

Figure 11: NPDCTB Deflection Profile under HDL for Various Beam Breath b_0 Values

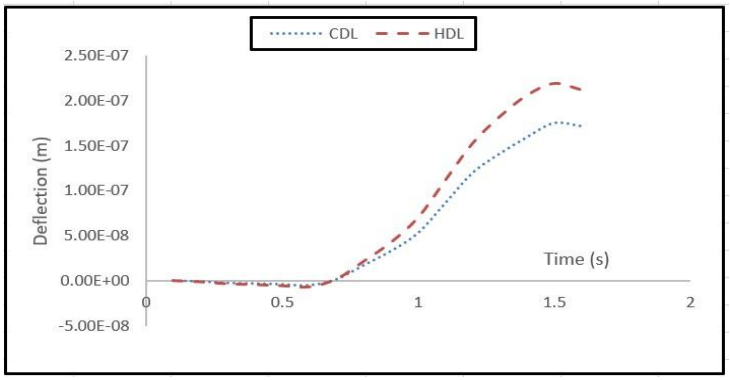

Figure 12: Comparison of CDL and HDL

The numerical results show that the dynamic response of an NPDCTB resting on an exponentially decaying foundation is strongly influenced by load speed, axial force, damping, and beam dimension (depth and breadth). Increases in load speeds increase deflection, while increases in axial force, damping, beam depth, and beam breadth reduce vibrations. HDL oscillations than CDL. These findings are applicable to the design of cantilever structures in bridges, offshore buildings, and some engineering structures, where controlling deflection and vibration is critical for safety and structural performance.

CONCLUSION

The NPDCTB resting on an exponentially decaying foundation was investigated in this research; the results show that load speed amplifies vibrations, while axial force, damping, and beam dimensions reduce deflections. The cantilever boundary and foundation decay strongly influence the dynamic behavior of NPDCTB, providing valuable insights for the design and optimization of cantilever structures in bridges, offshore buildings, and aerospace applications.

REFERENCES

Adedowole, A., and Famuagun, K. S. (2017). Influence of Exponentially Decaying Foundation on the Response of Non-Uniform Beams Under Uniformly Distributed Load. *American Journal of Innovative Research & Applied Sciences*. *5*(1), 77-87.

Adekunle, J. S., and Folakemi, A. O. (2017). Dynamic Response of Non-Uniform Elastic Structure Resting on Exponentially Decaying Vlasov Foundation under Repeated Rolling Concentrated Loads. *Asian Research Journal of*

Mathematics. 6(4): 1-11. https://doi.org/10.9734/ARJOM/2017/35785.

Alimi, A., and Adekunle, J. S. (2018). Dynamics analysis of a damped non uniform beam subjected to loads moving with variable velocity. *Archives of Current Research International*. *13*(2), 1-16. https://doi.org/10.9734/ACRI/2018/35919.

Al–Raheimy, N. H., and Hammed, L. (2022). Free Transverse Vibrations of Cantilever Beam for Tapered Thickness Prepared from Variant Fibers Reinforced Polyester. *Journal of the Serbian Society for Computational Mechanics. 16*(2), 1-12. https://doi.org/10.24874/jsscm.2022.16.02.01

Auricchio, F., Balduzzi, G., and Lovadina, C. (2015). The dimensional reduction approach for 2D non-prismatic beam modelling: a solution based on Hellinger–Reissner principle. *International Journal of Solids and Structures*. *63*, 264-276. https://doi.org/10.1016/j.ijsolstr.2015.03.004.

Bauchau, O. A., and Craig, J. I. (2009). *Structural analysis: with applications to aerospace structures* (Vol. 163). Springer Science and Business Media. https://doi.org/10.1007/978-90-481-2516-6_8

Clough, R. W., and Penzien, J. (1993). Dynamics of Structures. 2nd edn McGraw-Hill. *New York*, 195-200.
Dado, M., & Al-Sadder, S. (2005). A new technique for large deflection analysis of non-prismatic cantilever beams. *Mechanics research communications*. *32*(6), 692-703. https://doi.org/10.1016/j.mechrescom.2005.01.004.

Ece, M. C., Aydogdu, M., and Taskin, V. (2007). Vibration of a variable cross-section beam. *Mechanics Research Communications*. *34*(1), 78-84.

Elshabrawy, M., Abdeen, M. A., and Beshir, S. (2021). Analytic and numeric analysis for deformation of non-prismatic beams resting on elastic foundations. *Beni-Suef University Journal of Basic and Applied Sciences*. *10*(1), 57. https://doi.org/10.1186/s43088-021-00144-5

Fadugba, S. E., Shaalini, J. V., Ogunmiloro, O. M., Okunlola, J. T., and Oyelami, F. H. (2022, February). Analysis of exponential–polynomial single step method for singularly perturbed delay differential equations. *Journal of Physics: Conference Series* (Vol. 2199, No. 1, p. 012007). http://dx.doi.org/10.1088/1742-6596/2199/1/012007

Geraschenko, V. S., Grishin, A. S., & Gartung, N. I. (2018). Approaches for the calculation of Rayleigh damping coefficients for a time–history analysis. *Structures Under Shock and Impact XV*. *180*, 227-237.

Hashim, W. M., Alansari, L. S., Aljanabi, M., and Raheem, H. M. (2022). Investigating Static Deflection of Non-Prismatic Axially Functionally Graded Beam. *Material Design & Processing Communications*, *2022*(1), 7436024. https://doi.org/10.1007/s00707-022-03247-x

Inman, D. J. (2014). Engineering Vibration, New Jersey, Ed.
Jassim, Z. A., Ali, N. N., Mustapha, F., and Jalil, N. A. (2013). A review on the vibration analysis for a damage occurrence of a cantilever beam. *Engineering Failure Analysis*. *31*, 442-461. https://doi.org/10.1016/j.engfailanal.2013.02.016.

Jimoh, A., Ajoge, E. O. (2018). Influence of Damping Coefficient and Rotatory Inertia on the Dynamic Response to Moving Load of Non-Uniform Rayleigh Beam. *International Journal of Science, Engineering and Technology. 6(2), 139-149.* https://doi.org/10.2348/ijset02180139

Jimoh, A., and Ajoge, E. O. (2019). Dynamic analysis of Non-Uniform Rayleigh beam Resting on Bi-Parametric Subgrade under Exponentially Varying Moving Loads. *Journal of Applied Mathematics and Bioinformatics*. *9*(2), 1-16.

Lei, Y., Murmu, T., Adhikari, S., and Friswell, M. I. (2013). Dynamic characteristics of damped viscoelastic nonlocal Euler–Bernoulli beams. *European Journal of Mechanics-A/Solids*. *42*, 125-136. https://doi.org/10.1016/j.euromechsol.2013.04.006.

Li, X. F., Tang, A. A., and Xi, L. Y. (2013). Vibration of a Rayleigh cantilever beam with axial force and tip mass. *Journal of Constructional Steel Research*. *80*, 15-22. https://doi.org/10.1016/j.jcsr.2012.09.015

Ogbo, O. S., Momoh, E. O., Ndububa, E. E., and Adeshina, M. K. (2025). Analytical deflection modelling of symmetric non-prismatic reinforced laterite-concrete slabs. *Engineering Structures*. *334*, 120255. https://doi.org/10.1016/j.engstruct.2025.120255.

Ogunlusi, T. A., and Okafor, N. P. (2025). Vibration of Non-Prismatic Damped Thin Beam with Exponentially Varying Thickness Resting on Exponentially Decaying Foundations under Uniform Distributed Loads. *FUOYE Journal of Pure and Applied Sciences. 10*(2), 92-107. https://doi.org/10.55518/fjpas.AKPW3418

Ojih, P. B., Ibiejugba, M. A. and Adejo, B. O. (2014). Dynamic Response under moving concentrated loads of uniform Rayleigh beam resting on Pasternak foundation. *International Journal of Scientific and Engineering Research.* 5(6): 1-21.

Okafor, N. P., Ogunlusi, T. A., Ogunwe, F. T., and Ayobami, A. I. (2025). Dynamic Analysis of an Exponentially Decaying Foundation on the Response of Non-Uniform Damped Rayleigh Beam under Harmonic Moving Load with General Boundary Conditions. *Asian Research Journal of Mathematics*. *21*(1), 35-69. https://doi.org/10.9734/arjom/2025/v21i1882

Olotu, O.T., Omole, E.O. , Folaranmi., R.O., Yisa, B.M., Adeniran, P.O., and Gbadeyan, J.A. "Natural vibration analysis of axially graded tapered Rayleigh beams on a quadratic bi-parametric elastic foundation". *Nigerian Journal of Technology Development*, vol. 22, no. 1, pp. 79–94, 2025. https://doi.org/10.63746/njtd.v22i1.334

Omole, E. O., Ononogbo, C. B., Familua, A. B., Odeniyan-Fakuade, F. H., Folaranmi, R. O., Sunday, J., & Adeoye, A. S. (2025). Improved accuracy of fourth-order IVPs using the Taylor series block algorithms. *NIPES-Journal of Science and Technology Research*, 7(2, Special Issue: Landmark University International Conference SEB4SDG 2025), 4020–4035. https://doi.org/10.37933/nipes/7.4.2025.SI501.

Omolofe, B., Adedowole, A., Ajibola, S. O., and Ahmed, J. (2011). Exact Vibration Solution for initially stressed Beams

resting on Elastic Foundation and subjected to partially distributed masses. *Journal of the Nigerian Association of Mathematical Physics*. *18*, 91-98. https://doi.org/10.4314/jonamp.v18i1.

Oyelami, F. H., and Falodun, B. O. (2021). Heat and mass transfer of hydrodynamic boundary layer flow along a flat plate with the influence of variable temperature and viscous dissipation. *International Journal of Heat and Technology*. *39*(2), 441-450.. http://dx.doi.org/10.18280/ijht.390213

Praharaj, R. K., and Datta, N. (2022). Dynamic response spectra of fractionally damped viscoelastic beams subjected to moving load. *Mechanics Based Design of Structures and Machines*. *50*(2), 672-686. https://doi.org/10.1080/15397734.2020.1725563

Sarkar, K., Ganguli, R., and Elishakoff, I. (2016). Closed-form solutions for non-uniform axially loaded Rayleigh cantilever beams. *Struct. Eng. Mech*. *60*(3), 455-470.

Sunday, J., Omole, E. O., Ogunrinde, R. B., Kumleng, G. M., Bamisile, O. O., & Kayode, O. O. (2026). Mathematical formulation of a symmetry-compact three-step algorithm for computing the spatio-temporal generalized FitzHugh–Nagumo equations. *Symmetry*, 18(2), 324. ; https://doi.org/10.3390/sym18020324

Svedholm, C., Zangeneh, A., Pacoste, C., François, S., and Karoumi, R. (2016). Vibration of damped uniform beams with general end conditions under moving loads. *Engineering Structures*. *126*, 40-52. https://doi.org/10.1016/j.engstruct.2016.07.037.

Timoshenko, S. P., and Young, D. H. (1965). *Theory of structures*. McGraw-Hill.

Tolorunshagba, J. M. (2014). Response to moving variable concentrated load of non-uniform beams resting on exponentially decaying foundation. *Journal of Emerging Trends in Engineering and Applied Sciences*. 5(6), 378-383. https://hdl.handle.net/10520/EJC164599

Wu, J. S., and Chen, D. W. (2000). Dynamic analysis of a uniform cantilever beam carrying a number of elastically mounted point masses with dampers. *Journal of Sound and Vibration*. *229*(3), 549-578. https://doi.org/10.1006/jsvi.1999.2504.